Aksaray University
Journal of Science and Engineering

e-ISSN: 2587-1277
http://asujse.aksaray.edu.tr

Aksaray J. Sci. Eng.
Volume **9,** Issue **1,** pp. **35-44.**

Available online at DergiPark AKADEMİK

Research Article

Optical Characterization and Comparative Investigation of Cylindrical and Spherical Optical Microcavities

Gökçe DÜNDAR[1,4,*], Kerem Anar[2], Namık Akçay[3], Mustafa Eryürek[4]

[1] *İstanbul University, Institute of Graduate Studies in Sciences, Istanbul, Turkey*
[2] *Koç University, Department of Electrical&Electronics Engineering, Istanbul, Turkey*
[3] *İstanbul University, Faculty of Science, Department of Physics, Istanbul, Turkey*
[4] *TUBITAK BILGEM UEKAE, Gebze, Kocaeli, Turkey*

Keywords
Optical microcavity, Free spectral range (FSR), Quality factor (Q-factor), Whispering gallery mode (WGM), Tapered fiber

Article information
Received: Mar 5, 2025
Revised: Apr 22, 2025
Accepted: Mar 21, 2025
Online: Apr 28, 2025

doi: **10.29002/asujse.1650656**

Abstract
This study focuses on the optical excitation and characterization of cylindrical and spherical microcavities using tapered optical fibers. Optical microcavity technologies offer significant potential for optical sensing applications requiring ultra-high sensitivity. In this study, the interaction mechanisms between tapered fiber structures and microcavities were examined in detail, and the properties of so-called "whispering gallery mode" (WGM) resonances were analyzed. Cylindrical microcavities provide a sensitive sensing platform against environmental changes due to their simple geometric structures, while spherical microcavities stand out with their symmetrical shapes and higher quality factors (Q-factors). These structures play a critical role in enhancing spectral resolution and achieving precise measurements in optical sensing. In the experimental setup, adiabatic tapering techniques were employed to fabricate tapered optical fibers, and the efficiency of fiber-microcavity interactions was optimized. This setup allowed for resolving WGMs spectrally making precise measurement of Q-factors possible. Larger free spectral ranges (FSR) were obtained with cylindrical microcavities, whereas spherical microcavities achieved extremely high Q-factors with denser mode spectra. The results revealed the critical impact of geometric properties, fabrication quality, and alignment precision of microcavities on optical performance. This study provides a significant foundation for the integration of tapered fiber-based microcavities into advanced sensing technologies. In the future, optimizing fabrication techniques and system geometries could further enhance the sensitivity and performance of microcavities.

Anahtar Kelimeler
Optik mikrokovuk, Serbest spektral aralıklar (FSR), Kalite faktörü (Q-faktör), Fısıldayan galeri modları (WGM), İnceltilmiş fiber

Özet
Bu çalışma, inceltilmiş optik fiberler kullanılarak silindirik ve küresel mikrokovukların optik uyarımı ve karakterizasyonuna odaklanmaktadır. Optik mikrokovuk teknolojileri, çok yüksek hassasiyet gerektiren optik algılama uygulamalarında önemli bir potansiyel sunmaktadır. Bu çalışmada, inceltilmiş fiber yapıların mikrokovuklarla etkileşim mekanizmaları detaylı bir şekilde incelenmiş ve rezonans modlarının (WGM) özellikleri çözülmüştür. Silindirik mikrokovuklar, basit geometrik yapıları sayesinde çevresel değişikliklere karşı duyarlı bir algılama platformu sunarken, küresel mikrokovuklar şekilsel simetrileri ve daha yüksek Q-faktörleri ile öne çıkmaktadır. Bu yapılar, optik algılamada spektral çözünürlüğü arttırmak ve daha hassas ölçümler yapmak için kritik bir rol oynar. Deneysel düzenekte, inceltilmiş optik fiberlerin üretiminde adyabatik inceltme teknikleri kullanılmış ve fiber-mikrokovuk etkileşiminin verimliliği optimize edilmiştir. Bu düzenek, hem rezonans modlarının çözülmesine hem de Q-faktörünün hassas bir şekilde ölçülmesine olanak tanımıştır. Silindirik mikrokovuklarda daha büyük serbest spektral aralıklar (FSR) elde edilirken, küresel mikrokovuklar daha yoğun mod spektrumları ile çok yüksek Q-faktörlerine ulaşmıştır. Sonuçlar, mikrorezonatörlerin geometrik özellikleri, üretim kalitesi ve hizalama hassasiyetinin optik performans üzerindeki kritik etkisini ortaya koymuştur. Bu çalışma, inceltilmiş fiber tabanlı mikrokovukların ileri algılama teknolojilerine entegrasyonu için önemli bir temel sunmaktadır. Gelecekte, üretim tekniklerinin ve system geometrilerinin optimize edilmesi ile mikrokovukların duyarlılığını ve performansını daha da artırmak mümkün olabilecektir.

[*] ***Corresponding Author:*** *dundargokce90@gmail.com 0000-0002-7876-5818

1. Introduction

Optical microcavity technologies have gained significant attention in recent years due to their diverse applications across fields such as photonics, optoelectronics, biosensing and development of quantum computing components [1-3]. These structures, which confine light within a small volume, enhance light-matter interactions, leading to various advanced functionalities [4,5]. Additionally, optical microcavities play a crucial role in the miniaturization of optical filters, enabling higher precision in research and commercial technologies [6]. This light confinement allows nonlinear optics [7] and lasing [8] with WGMs. Moreover, there are other applications of optical microcavities such as chaotic behavior [9], high-frequency signal generation reaching up to THz levels [10], detection down to single molecules [11] and more [12,13].

The wavelength of the confined light is very sensitive to the dimensions of the microcavity, as well as the refractive indices of the microcavity and the environment [14]. Therefore, one of the primary applications of optical microcavities is optical sensing, where their high sensitivity allows the detection of minute changes in environmental conditions or concentration of biological agents. Over time, advancements in fabrication techniques have significantly improved the long-term stability and repeatability, as well as the Q-factor of these microcavities, improving the overall sensing performance of these devices [15-16].

Cylindrical and spherical microcavities fabricated using optical fibers have become a significant area of research due to their potential for achieving high Q-factors and enabling precise light confinement [17-18]. Moreover, the availability of the fibers makes producing these optical microcavities easy and low-cost. These fiber-based microcavities provide an efficient platform for enhancing light-matter interactions, which is critical for applications such as optical sensing, lasing, and telecommunication technologies [19]. The use of optical fibers allows for compact, integrated systems that maintain high performance while minimizing the size and complexity of the sensor [20]. Cylindrical microcavities exhibit WGMs because the light circulates along the outer boundary of the microcylinder. These WGMs have low losses and high Q-factors [21]. Spherical microcavities also support WGMs, but their symmetrical structure offers additional advantages in terms of mode distribution and sensitivity [22-24]. Recent advancements in controlled tapering of fibers enable the effective excitation of WGMs in these microcylinders or microspheres. Tapered fiber-microcavity structures offer a versatile platform for developing next-generation optical components with enhanced precision, tunability and sensitivity [25].

In this study, we focus on the fabrication of both cylindrical and spherical microcavities optically excited using tapered optical fibers. These microcavities demonstrate significant potential for high-precision optical sensing applications. Our work lays the groundwork for the future development of fiber-based optical microcavities and their integration into advanced sensing technologies.

2. Materials and Methods

2.1. Experimental Equipment

There are numerous methods to couple laser light to an optical microcavity. For instance, coupling of free-space laser light can be achieved using a focusing lens [26]. This method is easy to set up for excitation of the WGMs, but the coupling efficiency is low (<30%). Moreover, to collect the scattered light from the microcavity, another optical component must be used to direct the scattered intensity to a detector. Another method to excite an optical microcavity is to use a waveguide [27]. One way to couple the laser light in and out of the waveguide is end-face coupling between the fiber and the waveguide. End-face coupling has a low coupling efficiency, and it requires precise alignment between the fiber and the waveguide. For excitation of the microcavity and collection of the scattered light, two such end-face couplings are required. This further decreases the coupling efficiency and increases the complexity of the alignment. The overall coupling efficiency is less than 67% * 80% * 67% = 36% which is end-face coupling efficiency [28], waveguide to microresonator coupling efficiency [29] and once more end-face coupling efficiency, respectively. Higher coupling efficiency between a fiber and a waveguide can be achieved using the grating coupling method. However, grating structures with high coupling efficiency require patterning techniques with high resolution [30], and the requirement of precise alignment cannot be avoided using grating couplers. The usage of waveguides can be avoided if prism coupling is employed with a phenomenon called frustrated total internal reflection. Although the coupling efficiency may reach up to 80% [26], a precise alignment is needed for prism coupling [31].

In this study, tapered optical fibers were used to optically excite microcavities, since the tapered fiber coupling has the highest coupling efficiency which may reach over 99% [26]. Moreover, tapered fiber coupling is an economical and

practical method as compared with the other coupling methods with high coupling efficiency. The fiber tapering process was carried out using a hydrogen gas flame along with translation stages pulling the fiber in opposite directions, The tapering experiment utilized a single-mode optical fiber with an outer diameter of 125 µm and a core diameter of 8 µm. Before the tapering process began, the protective polymer coating on the outer surface of the fiber was stripped off which is succeded by cleaning the fiber with alcohol. Successful excitation of the optical microcavities required the fiber to be tapered down to a diameter of 2–3 µm to ensure strong light coupling into the microcavities from the tapered fiber. This is possible when the diameter of the taper becomes comparable to the wavelength of the excitation light (in our case ~1.55 µm) so that the evanescent field leaks out of the tapered fiber and excites the microcavity.

The fiber tapering setup was configured using Mdrive linear translation stages. To pull the fiber during the heating process, two motorized translation stages (Newport MPA-PP) and a motion controller (Newport ESP301) were employed. A hydrogen torch was used to apply localized heating to the fiber, while the linear translation stages moved at a controlled speed for a given distance. The system's movement resolution was set to 1024 steps per millimeter, allowing for precise control over the fiber tapering process. This level of resolution was crucial for achieving consistent and adiabatic tapering, which directly affects the coupling efficiency to the microcavities, especially in applications requiring high precision such as optical sensing.

As shown in Figure 1, the fiber was fixed between two translation stages and the fiber was heated using a hydrogen gas flame. The platforms were moved at a speed of 0.9 mm/s during the heating process, while the hydrogen gas flow rate was maintained at 0.34 slm. The combination of controlled heating and pulling allowed the fiber to be tapered adiabatically. Each translation stage was pulled for a distance of 11mm to achieve the diameter of the tapered section to be 2-3 µm. This level of precision in the tapering process is essential for achieving high Q-factors in the microcavities. After the pulling process was completed, the hydrogen flame was turned off and the translation stages were pulled further by a distance of ~300 µm to make the fiber taut.

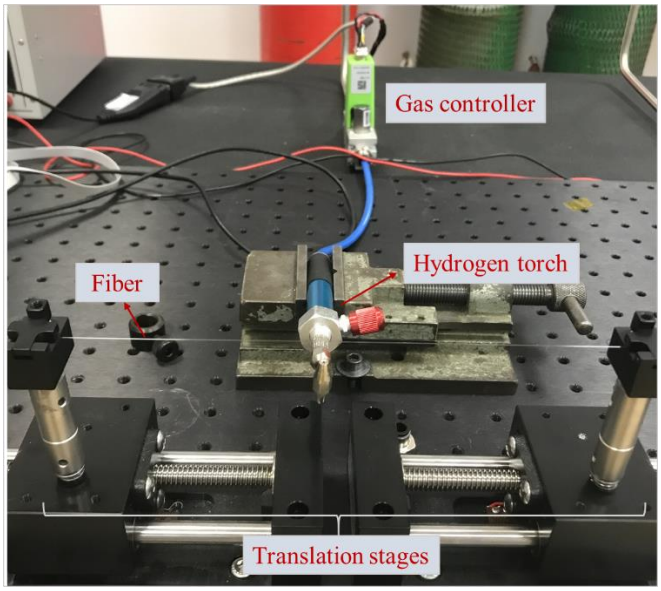

Figure 1. A photograph of the fiber tapering setup.

The speed, acceleration, and position of the motorized translation stages, as well as the hydrogen gas flow rate, were controlled using a computer. This level of automation ensured repeatability and consistency in the fiber tapering process. The use of hydrogen gas provides high enough temperatures for tapering to be successful.

By achieving such precise control over the tapering process, the optical excitation of the microcavities can be performed with high efficiency [32]. The tapering fibers served as a platform for the optical excitation of microcavity modes. This method of fiber tapering, coupled with the use of microcavities, has been shown in previous studies [16] to be highly effective in achieving high Q-factors, which are critical for enhancing the sensitivity and performance of optical sensors.

Certain wavelengths can be excited in the optical microcavities. These wavelengths depend on the geometrical parameters and the refractive index of the microcavity as well as the environmental conditions. To obtain these so-called "resonance" wavelengths, a tunable laser (Santec TSL-510-C, tunability range: 1500–1630 nm, wavelength resolution: 1 pm) is coupled into the tapered fiber and the tapered fiber is placed near the vicinity of the microcavity. As seen in Figure 6, these modes appear as peaks in the reflection spectrum of the microcavity. If a circulator is not used as in the case of

Figure 7, these modes can also be observed from the transmission spectrum as transmission dips. During the wavelength tuning process, the intensity of light passing through or reflected from the microcavity is recorded. This process is critical for identifying the resonant modes, which indicate the specific wavelengths where WGMs are efficiently confined within the microcavity.

The custom-developed software is designed to control the wavelength of the tunable laser, while simultaneously measuring the transmitted/reflected intensity. As the wavelength is tuned, the light intensity is measured using a photodiode, and the photodiode data is recorded in real-time using a data acquisition (DAQ) system. The ability to capture real-time data is essential for ensuring accurate mapping of the optical modes from the timestamp.

To ensure synchronization between the beginning of the wavelength tuning and the data collection in the photodiode, the laser's external trigger feature is employed. This ensures that all measurements are aligned with the wavelength sweep, reducing any potential timing errors.

This system provided a highly automated and precise method for scanning and analyzing the optical modes of the microcavities. The combination of a high-resolution tunable laser, real-time data collection, and customized software ensured that even subtle shifts in mode behavior can be detected. This is particularly important for applications in optical sensing, where minor changes in environmental conditions (such as refractive index variations) can cause measurable shifts in the resonant wavelengths. Similar systems have been used in previous studies to detect these changes with great accuracy, as demonstrated by Vahala [4], where tunable lasers and real-time data acquisition systems were crucial in obtaining high-sensitivity results.

2.2. Production of Cylindrical Microcavities

In this study, standard single-mode optical fiber (SMF-28) was used for the fabrication of cylindrical microcavities. The production process began by carefully stripping the polymer protective coating from the fiber. Once the protective coating was removed, the fiber is used as a cylindrical microcavity after it is placed near a tapered fiber (Figure 2).

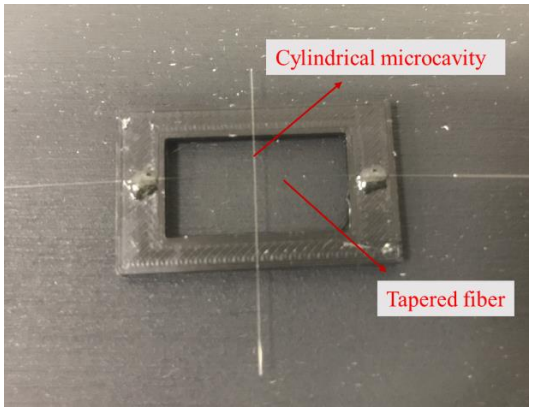

Figure 2. Cylindrical microcavity and the tapered fiber used for excitation of WGMs in the cylindrical microcavity.

Cylindrical microcavities offer specific advantages in optical sensing applications due to their ease of fabrication and ability to confine light along the outer boundary of the microcylinder. This confinement enables WGMs to propagate with minimal loss, enhancing the sensitivity of the cavity to changes in its surrounding environment, such as variations in the refractive index. Previous studies, such as those by Spillane [21], have demonstrated that cylindrical microcavities can achieve high Q-factors and exhibit excellent sensitivity, making them ideal for applications where precision and reliability are paramount.

2.2. Production of Spherical Microcavities

The production process began by carefully stripping the polymer protective coating from the fiber. After, the tip of the fiber was exposed to high temperatures using a hydrogen gas flame such that the tip of the fiber melted. During this process, the molten fiber naturally formed into a spherical shape due to the surface tension. Once the sphere was formed, its diameter was measured under a microscope and found to be approximately 460μm (Figure 3).

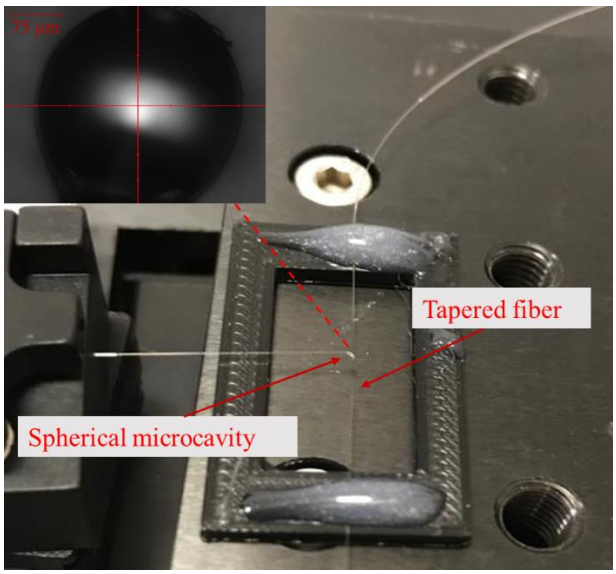

Figure 3. The spherical microcavity, the tapered fiber used to excite whispering gallery modes (WGMs) within the microcavity, and the microscopic image of this tapered fiber.

After fabrication, the spherical microcavity was carefully positioned and secured on the tapered fiber. Unlike the microcylinder, the placement of the microsphere affects the WGM spectrum dramatically. This is attributed to the fact that the microcylinder is symmetrical along the tapered fiber while the microsphere is not. Therefore the orientation and the location of the microsphere must be kept fixed with respect to the tapered fiber to obtain repeatable WGM spectra.

Spherical microcavities are known for their excellent ability to support WGMs with high Q-factors. These WGMs are highly sensitive to changes in the surrounding environment, making spherical microcavities ideal for optical sensing applications [24].

In this study, the spherical microcavities were meticulously analyzed, focusing on the characteristics and behaviors of the optical modes. The careful placement of the cavity on the tapered fiber, combined with precise mode scanning, allowed for the detailed observation of optical resonances.

2.4. Characteristic Properties of Microcavities: FSR and Q-factor

FSR refers to the wavelength or frequency difference between successive resonances or interference peaks in optical resonators and interferometers. In our case, FSR is defined to be difference in wavelengths of two successive resonance modes for a given microcavity. FSR depends on the geometrical parameters and refractive index of the microcavity as well as the wavelength of the excitation light [33].

For cylindrical resonators FSR is defined as follows [34];

$$FSR = \frac{\lambda^2}{2\pi r N_{eff}} \tag{1}$$

where λ is the wavelength of the excitation light, N_{eff} is the effective refractive index and r is the radius of the cylindrical microcavity.

For a spherical microcavity having a refractive index of N_{in} and residing in an environment of refractive index N_{out}, FSR [35];

$$FSR = \frac{\lambda^2}{2\pi r N_{out}} \frac{tan^{-1}\sqrt{(N_{in}/N_{out})^2-1}}{\sqrt{(N_{in}/N_{out})^2-1}} \tag{2}$$

FSR can be used as a verification method for the size of the microcavity. In cylindrical microcavities, FSR can be observed more clearly as opposed to the spherical microcavity. This is attributed to the different symmetries of the microcavities in which a spherical microcavity supports a higher number of modes making the identification of FSR harder than the cylindrical microcavities [36].

The quality factor (Q-factor) is a critical parameter in evaluating the performance of optical microcavities. It is calculated using the ratio of the resonance wavelength (λ_R) to the full width at half maximum (FWHM) of the curve of the resonance. The Q-factor serves as a crucial parameter in assessing the optical performance of microcavities, as it quantifies the ratio

of energy stored versus energy lost per cycle, thereby indicating the sensitivity and efficiency of the system. Generally, sensing with optical microcavities relies on the resonance shifts of WGMs. Therefore achieving high Q-factors allows more precise measurements.

The Q-factors of the cylindrical and spherical microcavities were calculated using the equation:

$$Q = \frac{\lambda_R}{\Delta\lambda_{FWHM}} \tag{3}$$

In this formula, λ_R represents the resonance wavelength, and $\Delta\lambda_{FWHM}$ denotes the FWHM of the resonance curve. The FWHM is calculated from the parameters obtained from the Gaussian fit applied to the resonance dip/peak. This method is widely used in analyzing the energy storage capacity and losses of optical resonators [37].

2.5. Experimental Setup

In this work, cylindrical and spherical microcavities are studied. To demonstrate the measurement is possible from both the scattering and the transmission configurations, the cylindrical microcavity is studied in the scattering configuration (Figure 4) whereas the spherical microcavity is studied in the transmission configuration (Figure 5). The only difference between the two configurations is, that a circulator is used to collect the scattered light in the scattering configuration. On the other hand, no circulator is needed for the transmission configuration. In the scattering configuration, the WGMs of the cylindrical microcavity are revealed as peaks (inset graph in Figure 4) whereas for the spherical microcavity, the WGMs are observed as dips (inset graph in Figure 5) because of the transmission configuration.

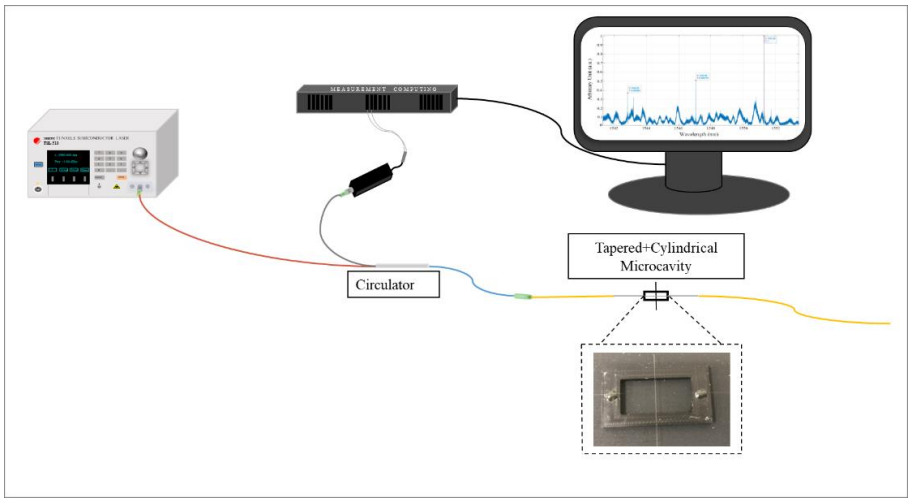

Figure 4. Experimental setup for mode measurements of the cylindrical microcavity. Since the data acquisition is collected from the reflected light from the cylindrical microcavity, the WGMs appear as peaks in the mode spectrum.

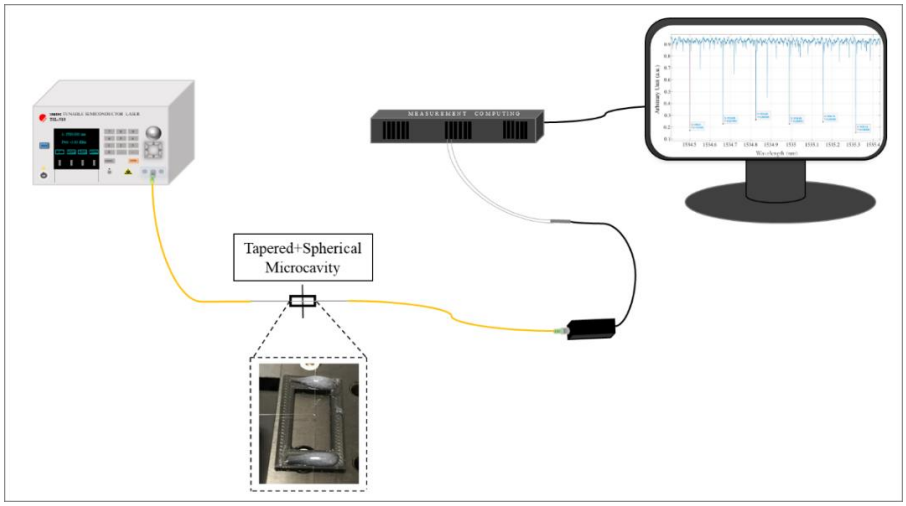

Figure 5. Experimental setup for mode measurements from the spherical microcavity. Since the data acquisition is collected from the transmitted light from the spherical microcavity, the WGMs appear as dips in the mode spectrum.

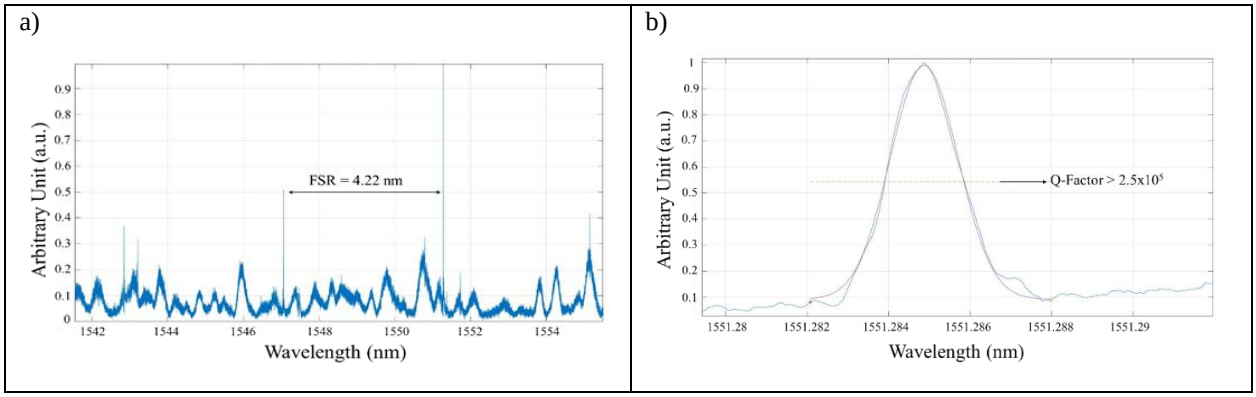

Figure 6. Modes of the cylindrical microcavity and their corresponding Q-factor values.

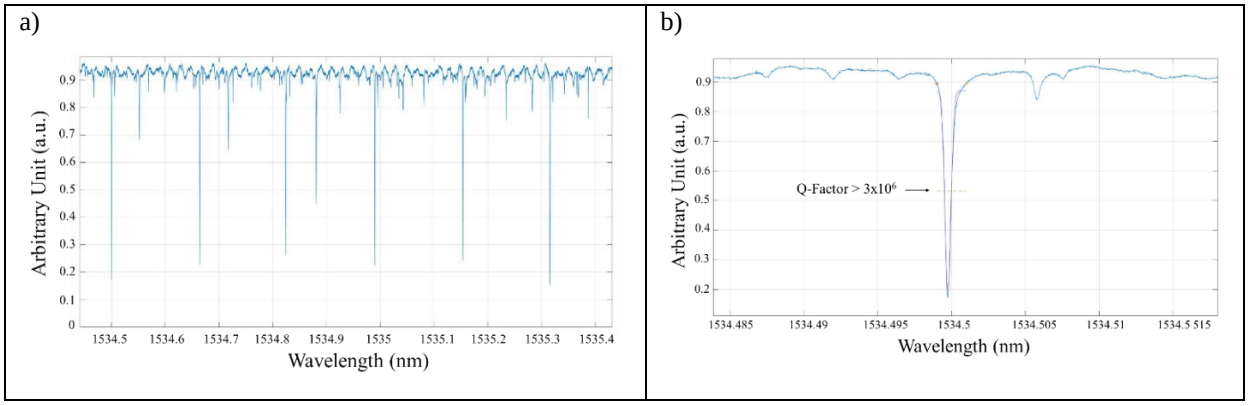

Figure 7. Modes of the spherical microcavity and their corresponding Q-factor values. FSR is not given because the WGM spectra of spherical microcavities are relatively crowded which makes it difficult to pinpoint the successive modes that give FSR.

3. Discussion of Results and Evaluation

In this study, optical characterization of cylindrical and spherical microcavities is demonstrated. For both microcavities, Q-factor measurements are performed. FSR measurement is only given for cylindrical microcavity. To excite the WGMs, tapered fibers are used. To demonstrate both reflection and transmission measurements are possible, WGM spectra of cylindrical microcavities are collected using a circulator. Therefore reflection spectra of cylindrical microcavities are obtained, making the WGMs appear as reflection peaks in the spectra (Figure 6). On the other hand, a circulator is not implemented for spherical microcavity measurements which makes WGMs of spherical microcavities appear as transmission dips in the spectra (Figure 7).

Q-factors of spherical microcavities are generally higher than that of cylindrical microcavities. In our measurements, the Q-factor is measured to be $>3x10^6$ for a spherical microcavity demonstrating exceptionally low optical losses and a high energy storage capacity (Figure 7b). This result highlights the system's ability to confine light efficiently, ensuring superior optical sensitivity and selectivity. The narrow and symmetric resonance curve confirmed that the resonance dip was successfully modeled using a Gaussian function. The Q-factor for a cylindrical microcavity is measured as $>2.5x10^5$ (Figure 6b). Although this value is lower than the spherical microcavity, it still demonstrates relatively low optical losses. This reduction can be attributed to increased scattering losses due to the difference in geometries of these microcavities. FSR of the cylindrical microcavity was calculated to be 4.22 nm (Figure 6a)**.** This is a much larger mode separation as compared with the spherical microcavity which shows a high spectral mode density **(**Figure 7a). Larger FSR can be advantageous in applications requiring reduced spectral overlap and mode isolation.

The differences between the spherical and cylindrical microcavities stem from their distinct geometrical properties and light confinement mechanisms. The spherical microcavity system offers higher Q-factors and smaller FSR values, making it well-suited for applications that demand high spectral resolution and sensitivity. In contrast, the cylindrical microcavity system, with its simpler geometry, ease of fabrication and larger FSR values, is ideal for applications where mode isolation and lower mode density are prioritized.

In conclusion, the results demonstrate that both spherical and cylindrical microcavity systems exhibit unique optical characteristics, with performance strongly influenced by geometry, alignment precision, and fabrication quality. Future studies should focus on optimizing the geometry and alignment of both systems to further reduce losses and improve the agreement between theoretical and experimental results. Addressing these factors will enhance the system's reliability and expand their potential applications in areas such as laser stabilization, optical filtering, and precision sensing [19]. These high Q-factor microcavities are also suitable for laser generation if they are doped with certain active ions [15].

Acknowledgments

This study was supported by the TUBITAK BIDEB [Project number 121C216].

References

[1] Toropov, N., Cabello, G., Serrano M.P., Serrano, R.R., Rafti, M., Vollmer, F., **(2021)**. *Review of biosensing with whispering-gallery mode lasers*, Light Sci Appl, 10,42. DOI: 10.1038/s41377-021-00471-3

[2] Notomi, M., Kuramochi, E., **(2008)**. *Large-scale arrays of ultrahigh-Q coupled nanocavities*, Nature Photon, 2: 741-747. DOI: 10.1038/nphoton.2008.226

[3] Aoki, T., Dayan, B., Wilcut, E., Bowen, W.P., Parkins, A.S., Kippenberg, T.J., Kimble, H.J., **(2006)**. *Observation of strong coupling between one atom and a monolithic microresonator*, Nature, 443: 671-674. DOI: 10.1038/nature05147

[4] Vahala, K.J., **(2003)**. *Optical microcavities*. Nature, 424: 839-846. DOI: 10.1038/nature01939

[5] Yang, J., Guo, LJ., **(2006)**. *Optical sensors based on active microcavities*. IEEE Journal of Selected Topics in Quantum Electronics, 12,1: 143–147. DOI: 10.1109/JSTQE.2005.862953

[6] Tang, G., Huang, Y., Chen, J., Li, Z., Liang, W., **(2022)**. *Controllable one-way add-drop filter based on magneto-optical photonic crystal with ring resonator and microcavities.* Optics Express, 30, 28762-28773. DOI:10.1364/OE.460271.

[7] Strekalov, D.V., Marquardt, C., Matsko, A.B., Schwefel, H.G.L., Leuchs, G., **(2016)**. *Nonlinear and Quantum Optics with Whispering Gallery Resonators.* Journal of Optics, 18, 123002. DOI: 10.1088/2040-8978/18/12/123002

[8] He, L., Özdemir, Ş.K., Yang, L., **(2013)**. *Whispering gallery microcavity lasers*. Laser Photonics Reviews, 7-1: 60-82.

[9] Tureci, H.E., **(2004)**. *Wave Chaos in Dielectric Resonators: Asymptotic and Numerical Approaches.* Doctoral Thesis. Corpus ID: 115383826

[10] Shioda, T., Yamazaki, T., **(2012)**. *Ultrafast optical frequency comb synthesizer and analyzer.* Optic Letters. 1;37(17):3642-4. DOI: 10.1364/OL.37.003642

[11] Armani, A.M., Kulkarni, R.P., Fraser, S.E., Flagan, R.C., Vahala, K.J., **(2007)**. *Label-Free, Single-Molecule Detection with Optical Microcavities.* Science, 317, 5839:783-787. DOI: 10.1126/science.1145002

[12] Ilchenko, V. S., Matsko, A. B., **(2006)**. *Optical resonators with whispering-gallery modes-part II: applications.* IEEE Journal of selected topics in quantum electronics, 12(1), 15-32. DOI: 10.1109/JSTQE.2005.862943

[13] Xiao, Y. F., Vollmer, F., **(2021)**. *Special Issue on the 60th anniversary of the first laser-Series I: Microcavity Photonics-from fundamentals to applications.* Light: Science & Applications, 10(1), 141. DOI: 10.1038/s41377-021-00583-w

[14] Eryürek, M., Karadag, Y., Ghafoor, M., Bavili, N., Cicek, K., Kiraz, A., **(2017)**. *Liquid refractometric sensors based on optical fiber resonators.* Sensors and Actuators A: Physical, 265, 161-167. DOI: 10.1016/j.sna.2017.08.019

[15] Lončar, M., Yoshie, T., Scherer, A., Gogna, P., Qiu, Y., **(2002)**. *Low-threshold photonic crystal laser*. Applied Physics Letters, 81(15): 2680-2682. DOI: 10.1063/1.1511538

[16] Maker, A.J., Armani, A.M., **(2012)**. *Fabrication of silica ultra high quality factor microresonator*, Journal of Visualized Experiments, 65:1-6. DOI: 10.3791/4164

[17] Yan, M., Zhang, X., Wang, J., Hou, F., Yang, L., Sun, W., Yang, Y., Wang T., **(2019)**. *Effects of end surface and angle coupling on mode splitting and suppression in a cylindrical microcavity.* Applied Optics, 58,7: 1752-1756. DOI: 10.1364/AO.58.001752.

[18] Ward, J., Benson, O., **(2011)**. *WGM microresonators: sensing, lasing and fundamental optics with microspheres*. Lazer Fotonik Rev, 5, 4: 553–570. DOI: 10.1002/lpor.201000025

[19] Vollmer, F., Arnold, S., **(2008)**. *Whispering-gallery-mode biosensing: label-free detection down to single molecules*. Nature Methods, 5(7): 591-596. DOI: 10.1038/nmeth.1221

[20] Brambilla, G., Finazzi, V., Richardson, DJ., **(2004)**. *Ultra-low-loss optical fiber nanotapers.* Optics Express, 12(10):2258-2263. DOI: 10.1364/OPEX.12.002258

[21] Tong, L., Gattass, RR., Ashcom, JB., He, S., Lou, J., Shen, M., Mazur, E., **(2003)**. *Subwavelength-diameter silicawires for low-loss optical waveguiding.* Nature, 426: 816-819. DOI: 10.1038/nature02193

[22] Spillane, SM., Kippenberg, TJ., Painter, OJ., Vahala, KJ., **(2002)**. *Ideality in a fiber-taper-coupled microsphere resonator system for application to cavity quantum electrodynamics*. Physical Review Letters, 91(4), 043902. DOI: 10.1103/PhysRevLett.91.043902.

[23] Braginsky, V.B., Gorodetsky, M.L., Ilchenko, V.S., **(1989)**. *Quality-factor and nonlinear properties of optical whispering-gallery modes*. Physics Letters A, 137(7-8): 393-397. DOI: 10.1016/0375-9601(89)90912-2

[24] Matsko, A.B., Ilchenko, V.S., **(2006)**. *Optical resonators with whispering-gallery modes. Part II: Applications.* IEEE Journal of Selected Topics in Quantum Electronics, 12(1): 3-14. DOI: 10.1109/JSTQE.2005.862952

[25] Birks, T.A., Li, Y.W., **(1992)**. *The shape of fiber tapers.* Journal of Lightwave Technology, 10(4): 432-438, DOI: 10.1109/50.134196

[26] Cai, L., Pan, J., Hu, S., **(2020)**. *Overview of the coupling methods used in whispering gallery mode resonator systems for sensing.* Optics and Lasers in Engineering , 127, 105968. DOI: 10.1016/j.optlaseng.2019.105968

[27] Eryürek, M., Karadag, Y., Taşaltın, N., Kılınç, N., Kiraz, A., **(2015)**. *Optical sensor for hydrogen gas based on a palladium-coated polymer microresonator.* Sensors and Actuators B: Chemical, 212, 78-83. DOI: 10.1016/j.snb.2015.01.097

[28] Schiappelli, F., Kumar, R., Prasciolu, M., Cojoc, D., Cabrini, S., De Vittorio, M., Visimberga, G., Gerardino, A., Degiorgio, V., Di Fabrizio, E., **(2004)**. *Efficient fiber-to-waveguide coupling by a lens on the end of the optical fiber fabricated by focused ion beam milling.* Microelectronic Engineering, 73–74, 397-404. DOI: 10.1016/j.mee.2004.02.077.

[29] Savchenkov, A.A., Mahalingam, H., Ilchenko, V. S., Takahashi, S., Matsko, A. B., Steier, W. H., Maleki, L., **(2017)**. *Polymer Waveguide Couplers for Fluorite Microresonators.* IEEE Photonics Technology Letters, 29(8): 667-670. DOI: 10.1109/LPT.2017.2675279.

[30] Taillaert, D., Van Laere, F., Ayre, M., Bogaerts, W., Van Thourhout, D., Bienstman, P., Baets, R., **(2006)**. *Grating Couplers for Coupling between Optical Fibers and Nanophotonic Waveguides.* Japanese Journal of Applied Physics, 45, 6071. DOI: 10.1143/JJAP.45.6071

[31] Vogt, D. W., Jones, A.H., Schwefel, H.G.L., Leonhardt, R., **(2018)**. *Prism coupling of high-Q terahertz whispering-gallery-modes over two octaves from 0.2 THz to 1.1 THz.* Optic Express, 26, 31190-31198. DOI: 10.1364/OE.26.031190

[32] Yariv, A., **(2000)**. *Universal relations for coupling of optical power between microresonators and dielectric waveguides*. Electronics Letters, 36(4): 321-322. DOI: 10.1049/el:20000340.

[33] Ozel, B., Nett, R., Weigel, T., Schweiger, G., Ostendorf, A., **(2010)**. *Temperature sensing by using whispering gallery modes with hollow core fibers.* Measurement Science And Technology, 21: 094015. DOI:10.1088/0957-0233/21/9/094015

[34] Kavungal, V., Farrell, G., Wu, Q., Mallik, A K., Semenova, Y., **(2018)**. *Studies of geometrical profiling in fabricated tapered optical fibers using whispering gallery modes spectroscopy*. Optical Fiber Technology, 41:82-88. DOI: 10.1016/j.yofte.2018.01.007

[35] Chýlek, P., Kiehl, JT., Ko, M.K.W., **(1978)**. *Optical levitation and partial-wave resonances*. Physical Review A, 18:2229-2233.

[36] Benner, H.E., Barber, P.W., Owen, F., Chang, B.K. **(1980)**. *Observation of Structure Resonances in the Fluorescence Spectra from Microspheres*. Physical Review Letters, Vol 44, No 7.

[37] Armani, A.M., Vahala, K., **(2006)**. *Heavy water detection using ultra-high-Q microcavities*. Optics Letters, 31:1896-1898.